A conceptual model for glacial lake bathymetric distribution

Taigang Zhang[1,2,3], Weicai Wang[1], Baosheng An[1,4]

[1]State Key Laboratory of Tibetan Plateau Earth System, Environment and Resources (TPESER), Institute of Tibetan Plateau Research,

Chinese Academy of Sciences, Beijing 100101, China

[2]College of Earth and Environmental Sciences, Lanzhou University, Lanzhou 730000, China

[3]Center for the Pan-Third Pole Environment, Lanzhou University, Lanzhou 730000, China

[4]School of Science, Tibet University, Lhasa 850011, China

Correspondence: Taigang Zhang (zhangtg16@lzu.edu.cn) and Weicai Wang (weicaiwang@itpcas.ac.cn)

Abstract. The formation and expansion of glacial lakes worldwide due to global warming and glacier retreat have been well documented in the past few decades. Thousands of glacial lake outburst floods (GLOFs) originating from moraine-dammed and ice-dammed lakes were reported, causing devastating impacts on downstream lives and properties. Detailed glacial lake bathymetry surveys are essential for accurate GLOF simulation and risk assessment. However, these bathymetry surveys are still scarce as glacial lakes located in remote and high-altitude environments hamper a comprehensive investigation. We developed a conceptual model for glacial lake bathymetric distribution using a semi-automatic simulation procedure. The basic idea is that the statistical glacial lake volume-area curves conform to a power-law relationship indicating that the idealized geometric shape of the glacial lake basin should be hemispheres or cones. First, by reviewing the evolution of various types of glacial lakes, we identified 9 standard conceptual models to describe the shape of lake basins. Second, we defined a general conceptual model to depict the continuum transitions between different standard conceptual models for those specific glacial lakes that lie between two standard conceptual models. Third, we nested the optimal conceptual model into the actual glacial lake basin to construct the water depth contours and interpolate the glacial lake bathymetric distribution. We applied the conceptual model to simulate six typical glacial lakes in the Third Pole with in-situ bathymetric surveys to verify the algorithm's applicability. The results show a high consistency in the point-to-point comparisons of the measured and simulated water depths with a total volume difference of approximately ±10%. The conceptual model has significant implications for understanding glacial lake evolution and modeling GLOFs in the future.

1 Introduction

Globally, glacial recession and thinning have been well-documented over the last decades via field observations and remote sensing techniques (Yao et al., 2012; Zemp et al., 2019; Hugonnet et al., 2021). Such evolution of glaciers due to climate warming and anthropogenic factors could induce related effects (Yao et al., 2019), among which is the expansion and formation of glacial lakes (Zhang et al., 2015; Emmer et al., 2016; Wang et al., 2020; Ma et al., 2021). Glacial lakes are water bodies developed within depressions of glacier moraine or mainly fed by contemporary glacier meltwater (Yao et al., 2018). Due to glacier retreats, they are generally impounded by glacier terminal or lateral moraine. Since the 1990s, the glacial lakes within 1 km buffer of the contemporary glaciers worldwide have increased by around 50% in total number, area, and volume (Shugar et al., 2020). These changes have also been accompanied by glacial lake outburst flood (GLOF) risks.

As a glacier–related hazard, GLOF has been a frequent incidence in various glacierized areas, causing considerable socioeconomic losses (Anacona et al., 2015a; Nie et al., 2018; Emmer et al., 2022a). According to a compilation, more than 3,000 GLOFs from moraine- and ice-dammed lakes are recorded worldwide and claim more than 10,000 deaths (Carrivick and Tweed, 2016; Lützow et al., 2023). Under the triggering factors such as ice avalanches, landslides, and heavy precipitation, glacial lakes are extremely unstable and subsequently cause a sudden release of water with peak discharge higher than a dozen times that of monsoon rainfall floods (Richardson and Reynolds, 2000; Westoby et al., 2014; Kougkoulos et al., 2018). However, due to the relatively small volume of the glacial lake, the flooding process generally attenuates rapidly within a few hours. Knowledge of glacial lake volume is critical, as it influences the released water volume and GLOFs magnitude (Fujita et al., 2013). Therefore, lake volume is often employed as an essential criterion in numerous cases of GLOF susceptibility and risk assessment (Bolch et al., 2011; Aggarwal et al., 2017; Drenkhan et al., 2019; Falatkova et al., 2019).

Currently, only sporadic bathymetric surveys on glacial lakes have been conducted worldwide. In Cordillera Blanca, Peru, facing continuous threats by GLOFs (Lliboutry et al., 1977), more than 100 detailed bathymetric surveys of glacial lakes have been carried out to better understand the regional GLOF risks (Muñoz et al., 2020). Government agencies and research institutions have promoted these surveys. In the Third Pole region, the bathymetric surveys are focused on the glacial lakes in the Himalayas (Sharma et al., 2018; Watson et al., 2018), where approximately 60 bathymetric surveys of glacial lakes, such as the Cirenmaco, Jialongco, and Longbasaba Lake, were conducted (Yao et al., 2012; Wang et al., 2018; Li et al., 2021). They measure the water depth with ultrasonic

57 devices onboard automatic uncrewed boats or manual hovercrafts.

58   Performing a universal investigation campaign of lake bathymetry is impractical for thousands of glacial lakes

59 in remote areas and high elevations. Instead, scholars typically utilize single total lake volume data rather than

60 bathymetric distribution in GLOF modeling (Anacona et al., 2015b; Zhang et al., 2021). The lake volume is typically

61 estimated by empirical equation, e.g., direct volume–area equation (O'Connor et al., 2001; Huggel et al., 2002;

62 Loriaux and Casassa, 2013), or indirect area–mean depth/maximum depth/width equation (Wang et al., 2012), which

63 have considerable uncertainty. There is no doubt that the measured and/or interpolated glacial lake bathymetric

64 distribution have great merit that can precisely determine the maximum potential outburst volume of the glacial lake,

65 serving to further simulate the GLOF propagation and evaluate downstream exposures (Frey et al., 2018; Sattar et

66 al., 2021). Moreover, a bathymetry survey is also pivotal to understand the interactions between the glaciers and their

67 terminating lakes (Zhang et al., 2023), as several studies have revealed that the proglacial lake bathymetric state can

68 dominate the glacier terminal melting and calving regimes (Watson et al., 2020; Sugiyama et al., 2021).

69   Can we obtain glacial lake bathymetric distributions through modeling rather than in situ investigations?

70 Previous studies have provided insights. Cook and Quincey (2015) preliminarily proposed that the same type of

71 glacial lakes may have their idealized geometric shapes, which depict the evolution of glacial lakes' volume–area (V–

72 A) relationship over time. For instance, the triangular cone is suitable to represent the idealized geometric shape of

73 ice-dammed lakes dammed by glaciers and formed in the narrow valley. The idealized conceptual models of glacial

74 lakes can be combined with the actual situations to project the glacial lake bathymetric distribution.

75   An idealized lake basin is also helpful in constructing numerical or physical models. In the study of Veh et al.

76 (2020), the conceptual model of glacial lakes was constructed as a semi-ellipsoid with a circular surface to calculate

77 the released volume after the lake drainage. The surface area and height of the semi-ellipsoid refer to the glacier lake

78 area and maximum water depth, respectively. Based on these instructive designs, we attempted to develop a procedure

79 and algorithm for modeling glacial lake bathymetric distribution in this study. We first (i) retrieved as many as

80 possible conceptual models for various types of glacial lakes by reviewing the evolutions of glacial lakes and

81 analyzing the relationships between lake volumes and areas; (ii) explored the procedure and algorithm to estimate

82 bathymetric distribution in conjunction with actual lake surface and basin shapes; and then (iii) discussed their

83 implications and potential applications.

84 **2   Data and methods**

2.1 Compilation of glacial lake bathymetry

Analyzing the existing glacial lake bathymetries can help us reveal glacial lake water depth characteristics. To our knowledge, more than 60 articles have mentioned surveyed bathymetry data from glacial lakes. We integrated the prior studies and established an inventory of global glacial lake bathymetry (Supplementary material 1). The attributes included the name, location, survey time, area, volume, and maximum water depth. A total of 231 bathymetric data from 220 glacial lakes globally were compiled in the inventory (Fig. 1a). Some large glacial lakes were eliminated since their area deviate from the majority of concentration zone which could reduce the fitting accuracy (Cook and Quincey, 2015).

2.2 Classification and evolution of different glacial lake types

The maximum water depth (D) and total volume (V) are the fundamental parameters regarding the idealized geometric shape of glacial lakes. We used the compiled glacial lake bathymetry data to fit the curves of V–A (glacial lake area) and D–A to understand the potential shapes of an idealized lake basin. Based on the topological positions between the glacial lakes and their parent glaciers, we classified glacial lakes as proglacial, periglacial, extraglacial, supraglacial, and ice-dammed types (Fig. 1b). This classification system considers glaciers' critical role in the evolution of glacial lakes (Petrov et al., 2017; Rick et al., 2022).

We assumed that different types of glacial lakes have different expansion mechanisms and, thus, different conceptual models (Carrivick and Tweed, 2013; Mertes et al., 2017; Minowa et al., 2023). The proglacial lake's expansion mainly proceeds backward by glacial retreat (Minowa et al., 2023). For instance, Longbasaba Lake, located in the central Himalayas, has substantially increased its surface area by occupying space liberated through glacier terminal retreat since 1988, with limited expansion in the frontal and lateral moraine areas (Wei et al., 2021). The periglacial lake and the extraglacial lake are not directly in contact with the glacier, and their expansion depends more on changes in precipitation and glacier meltwater, thereby potentially expanding in all horizontal directions. As for the supraglacial lake, expansion proceeds in all directions, and the temperature difference at the ice-water interface continuously melts the glacier ice in both horizontal and vertical orientations (Watson et al., 2018). While for ice-dammed lake, the evolution often appears horizontally with glacier retreat, as seen in the expansion of Merzbacher Lake in the Tianshan Mountains (Gu et al., 2023). These various mechanisms in glacial lake expansions showed that the changes in the lake basin among the different glacial lake types are inconsistent, indicating that they may have different conceptual models.
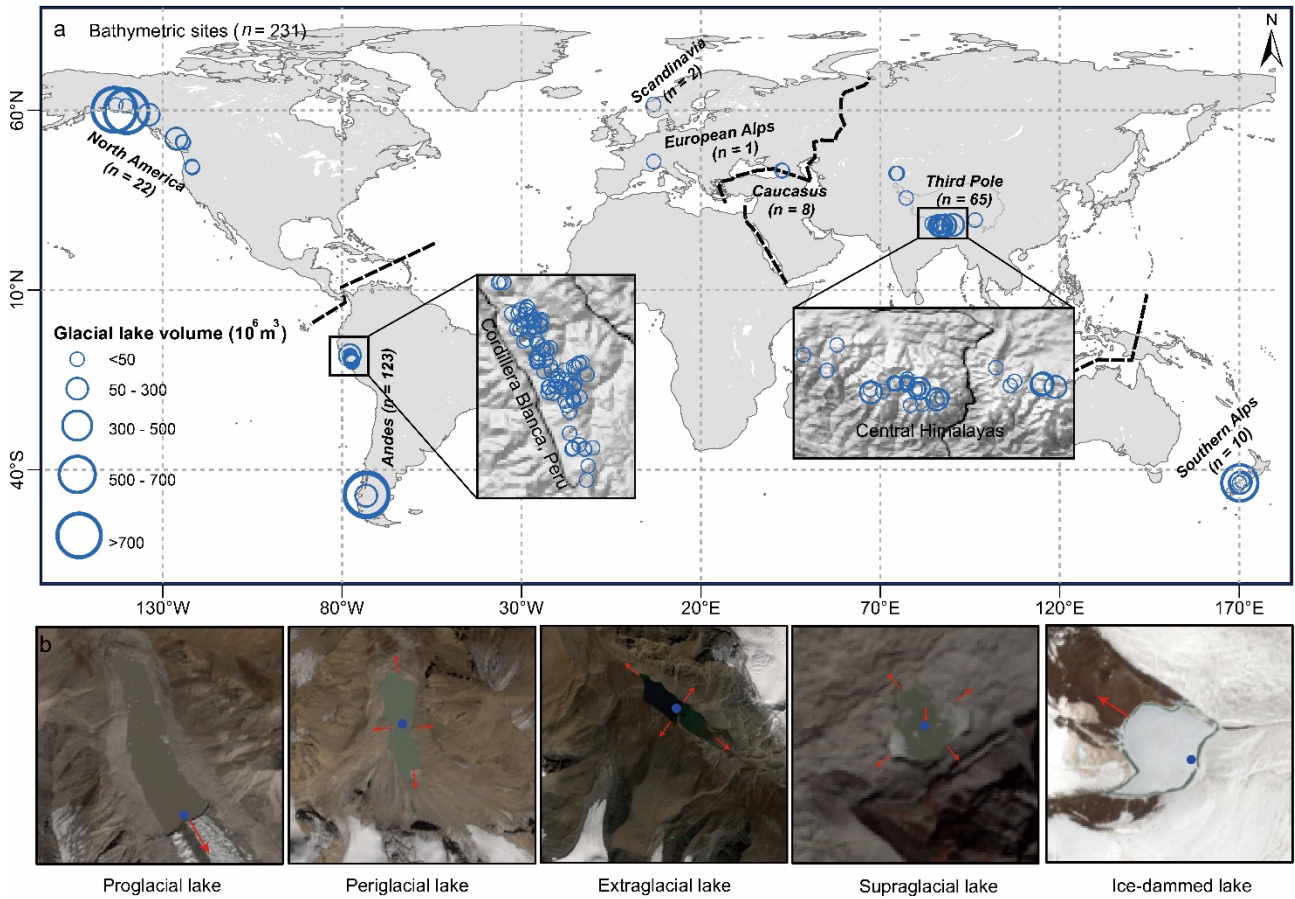
Figure 1. (a) Distribution of glacial lakes whose volume was surveyed in detail. (b) Glacial lakes were divided into five categories, namely proglacial (direct in contact with glacier terminus), periglacial (separated from the glacier and dammed by historical moraine), extraglacial (far from the glacier and generally dammed by landslides), supraglacial (positioned on the glacier surface), and ice-dammed lake (formed when glacier surges block downstream valleys or meltwater fills depressions between retreating tributary and main glaciers). Red arrows indicate the possible main directions of expansion of the glacial lake, and the blue points represent the location of maximum water depth. Credit: Copernicus Sentinel data.

2.3 Standard conceptual model

The basic procedure of constructing glacial lake bathymetric distribution is to (i) identify the most appropriate conceptual model that can describe the idealized lake basin, (ii) calculate the theoretical formulation equations of this conceptual model, (iii) nest this conceptual model into the actual glacial lake basin to construct the water depth contours, and (iv) interpolate and calculate the glacial lake bathymetric distribution. The conceptual model was constructed as the scheme presented by Veh et al. (2020). Glacial lakes were assumed to have hemispherical or similar

three-dimensional lake basin shapes. The standard surface of the glacial lake was assumed to be an ellipse.

The general formula between the volume and area of glacial lakes fits a power-law relationship (Table 1). It could be expressed as Eq. (1). The best-fit curve for the relationship between maximum water depth and area of glacial lakes also follows the power-law relationship (Eq. 2) (Fig. 2).

$$V = \alpha A^{\beta} \qquad (1)$$

$$D = \gamma A^{\varepsilon} \qquad (2)$$

A is the area of the glacial lake; α, β, γ, and ε are the coefficients. The value of β is greater than 1, and ε is less than 1.

The three-dimensional bodies representing the standard shape of a lake basin were required to have a general formula as defined by Eq. (3):

$$V = \delta AD \qquad (3)$$

Here, δ is the coefficient, A is the elliptical surface area, and D corresponds to the maximum water depth of the glacial lake. We identified four hemispheres or cones whose volumes can be expressed by Eq. (3): the hemisphere structured by the elliptical side ($V = 2/3AD$); the hemisphere structured by the upward-opening parabolic side ($V = 1/2AD$); the cone structured by the straight side ($V = 1/3AD$); and the cone structured by the rightward-opening parabolic side ($V = 1/5AD$). These bodies are defined as the standard conceptual model (SCM), and their curves in the X-O-Z quadrant are called the standard curves (Fig. 3a). These four standard curves are progressively concave inward in the quadrant, from the elliptical curve to the rightward-opening parabolic curve.

These SCMs for the supraglacial, periglacial, and extraglacial lakes are compatible with the expansion mechanisms partly because their growth direction is comprehensive at the horizontal level. Their maximum water depths were set in the lake center. However, proglacial and ice-dammed lakes are different. Their expansions are focused toward the glacier's or valley's direction, and the maximum water depths are generally situated near the intersection with the glacier, e.g. Longbasaba proglacial lake (Yao et al., 2012; Wei et al., 2021) and Shisper ice-dammed lake (Singh et al., 2023). Under these circumstances, we considered the SCMs of proglacial lakes to be half of the preceding four SCMs, namely the semi-hemisphere structured by the elliptical side ($V = 1/3AD$); the semi-hemisphere structured by the upward-opening parabolic side ($V = 1/4AD$); semi–cone structured by the straight side ($V = 1/6AD$); and the semi-cone structured by the rightward-opening parabolic side ($V = 1/10AD$). We designed two

154   SCMs for the ice-dammed lake (Fig. 3a): the semi–cone structured by the straight side ($V = 1/6AD$) and the triangular

155   cone ($V = 1/3AD$). The deepest point for proglacial and ice-dammed lake were set near the glacier-lake interface.

156   Most of the actual volume points lie between the volume curves of these SCMs (Fig. 4), and there are one or two

157   closer SCM volume curves for each type of glacial lake's fitted A–V curve. Ultimately, a total of 9 different SCMs

158   were designed to express the idealized geometric shapes of glacial lake basin.

159

160   **Table 1.** Empirical equations of volume and area of glacial lakes in previous studies. The applicable region, lake type, and sample size

161   for each empirical equation were indicated during fitting. The volume unit is $10^6\,\text{m}^3$, and the area unit is km^2. In the dam material-

162   based classification method for glacial lakes, a substantial number of proglacial and periglacial lakes can be categorized as moraine-

163   dammed lakes.

| ID	Empirical formulas	Region	Lake types	Samples	Reference
1	$V = 35A^{1.5}$	British Columbia, Canada	Ice-dammed lake	not mentioned	Evans, 1986
2	$V = 168.5A^2 + 3.11A$	Northwestern America	Moraine-dammed lake	7	O'Connor et al., 2001
3	$V = 34.44A^{1.42}$	Worldwide	Moraine- and ice-dammed lake	13	Huggel et al., 2002
4	$V = 43.24A^{1.53}$	Himalayas	Moraine-dammed lake	17	Sakai, 2012
5	$V = 6.07A^{1.37}$	Himalayas	Moraine-dammed lake	20	Wang et al., 2012
6	$V = 55A^{1.25}$	Himalayas	Moraine-dammed lake	20	Fujita et al., 2013
7	$V = 33.58A^{1.39}$	Worldwide	Moraine- and ice-dammed lake	31	Loriaux and Casassa, 2013
8	$V = 42.93A^{1.48}$	Peruvian Andes	Moraine- and bedrock-dammed lake	35	Emmer and Vilímek, 2014
9	$V = 34.07A^{1.37}$	Worldwide	Various types	69	Cook and Quincey, 2015
10	$V = 11.49A^{1.26}$	Worldwide	Supraglacial lake	9	Cook and Quincey, 2015
11	$V = 60A - 6.28$	Worldwide	Moraine-dammed lake	42	Cook and Quincey, 2015
12	$V = 2.63e^A$	Worldwide	Ice-dammed lake	9	Cook and Quincey, 2015
13	$V = 37.3A^{1.47}$	Himalayas	Moraine-dammed lake	33	Khanal et al., 2015
14	$V = 52.2A^{1.18}$	Himalayas	Proglacial lake	6	Sharma et al., 2018
15	$V = 40A^2 + 5.06A$	Himalayas	Moraine-dammed lake	17	Patel et al., 2017
16	$V = 35.36A^{1.47}$	Central Asia	Moraine-dammed lake	32	Kapitsa et al., 2017
17	$V = 32.13A^{1.49}$	Himalayas	Ice-dammed lake, supraglacial lake	not mentioned	Miles et al., 2018
18	$V = 28.95A^{1.33}$	Worldwide	Moraine-dammed lake	93	Watson et al., 2018
19	$V = 35.46A^{1.4016}$	Himalayas	Supraglacial lake	24	Watson et al., 2018
19	$V = 41WA + 2A$	Cordillera Blanca, Peru	Moraine-dammed lake	120	Muñoz et al., 2020
20	$V = 37.36A^{1.41}$	Peruvian Andes	Various types	170	Wood et al., 2021
21	$V = 38.04A^{1.36}$	Peruvian Andes	Moraine-dammed lake	not mentioned	Wood et al., 2021
22	$V = 43.27A^{1.64}$	Peruvian Andes	Unclassified	not mentioned	Wood et al., 2021

164
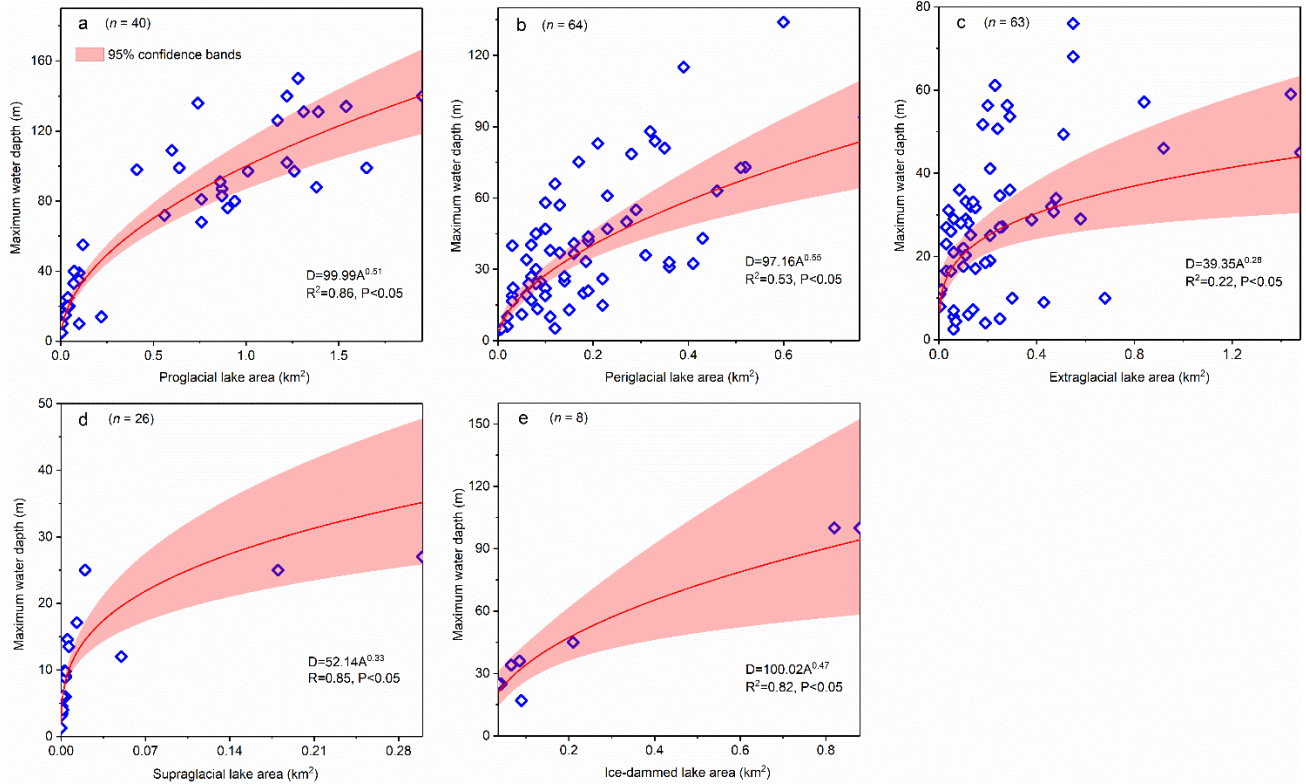
Figure 2. Relationships between maximum water depth and the area of glacial lakes were compiled in the present study for the following

lake types: (a) proglacial lake, (b) periglacial lake, (c) extraglacial lake, (d) supraglacial lake, and (e) ice-dammed lake.
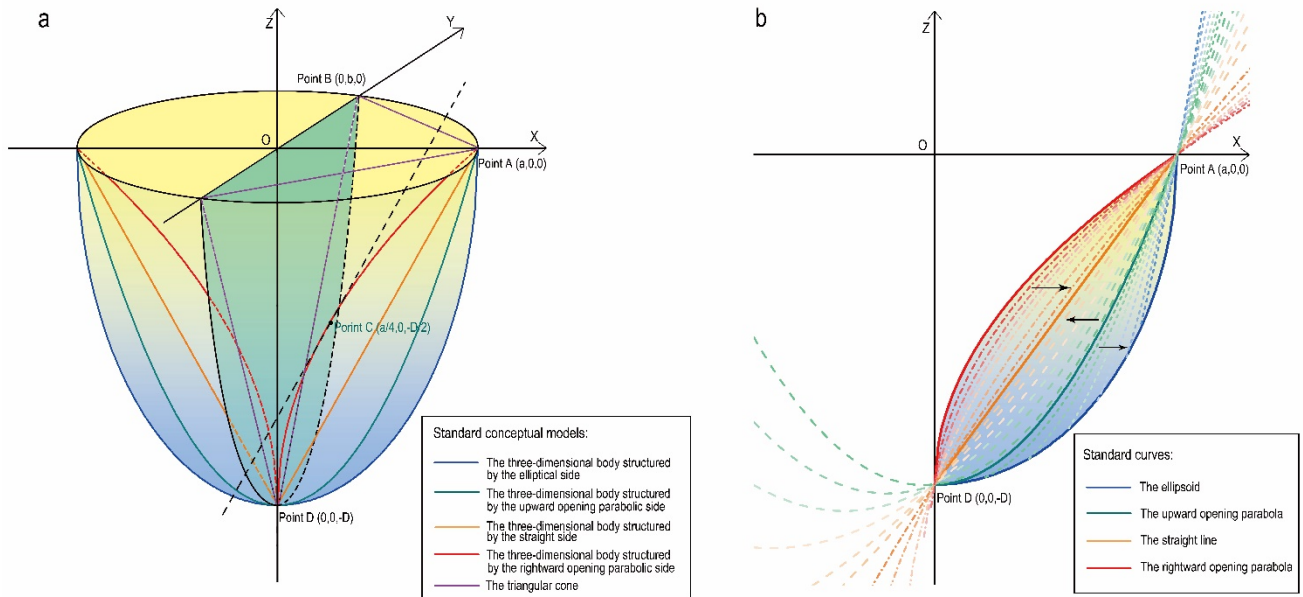

Figure 3. (a) Schematic diagram illustrates the shapes of the SCMs, namely the hemisphere structured by the elliptical side/upward-

opening parabolic side, the cone structured by the straight side/rightward-opening parabolic side, the triangular cone, as well as their

shapes when symmetrically divided matching the SCMs of the proglacial lake. Here, A is the semi-long axis, B is the elliptical surface's

semi-short axis, and D is the maximum water depth. (b) Convergences of the general curves towards the standard curves in the X–O–Z

173   quadrant in different orientations.
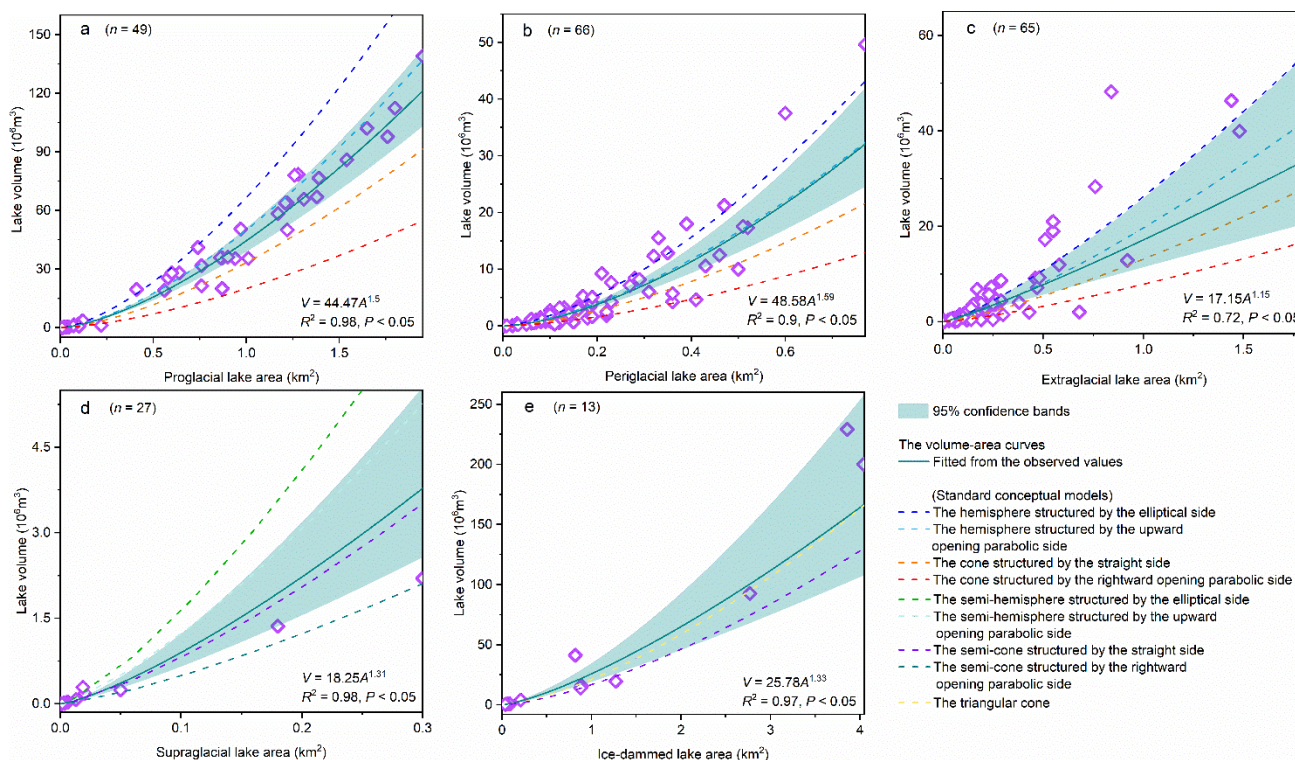
Figure 4. Relationships between the volume (V) and area (A) of glacial lakes were compiled in the present study for the following lake
types: (a) proglacial lake, (b) periglacial lake, (c) extraglacial lake, (d) supraglacial lake, and (e) ice-dammed lake. The dotted lines
indicate the volume curves of different standard conceptual models, which were fitted by Eq. (2) and (3).

2.4   General conceptual model

179   If a specific glacial lake has determined its parameters such as surface size, maximum water depth, and volume,

180   it is unlikely that the closest SCM would accurately represent the most appropriate conceptual model. This is because

181   the relatively inherent volume of the SCM is hardly equal to the volume of a specific glacial lake. In other word, the

182   volume curve of the SCM is constant, and therefore, the volume point of a specific glacial lake may deviate from the

183   SCM volume curve. Consequently, directly using the SCM to nest and interpolate a realistic glacial lake bathymetric

184   distribution would result in an initial over- or underestimation of the total lake volume.

185   The SCMs can only help us comprehend the various glacial lake morphologies; they cannot be applied directly

186   to estimate the glacial lake bathymetric distribution. We may conceive the measured volume points between the SCM

187   volume curves as a result of the transition from one SCM to another. For instance, from the upward-opening parabolic

188   line to the straight line, it is the standard parabolic line continuously approximating the straight line on the X–O–Z

quadrant by moving downward and left (Fig. 3b). During the movement process, the rotated–out hemisphere is moving toward the cone structured by the straight side. We can capture these general conceptual models (GCMs) in this transition stage and make their volume consistent with the measured or estimated lake volume. This means we find a GCM that is more effective than the SCM in estimating the lake depth distribution.

Python programming was used to drive the standard curves' transition and parameter calculations. The theoretical description for the GCMs is presented in supplementary material 2. By relocating the standard curve's vertices and altering the opening size, it is simple to compute the transition of a standard upward/rightward-opening parabola to a straight line. The resultant general curves must pass through points A and D. The convergence to the standard elliptic curve from the standard upward-opening parabola is relatively complicated. If we move the vertices of the standard parabola to the right and downward, the maximum height of the produced GCM changes. We used a compound style here. When the second intersection of the moved general parabolic curve and the standard elliptic curve occurs (from right to left), the side of GCM starts to take the elliptic curve change. Additionally, the marginal SCMs should be employed when the measured volume is larger (smaller) than the largest (smallest) SCM volume.

2.5 Nesting the actual glacial lake shapes

Once a given glacial lake's GCM has been established, the lake's bathymetric contours may be predicted in relation to actual conditions and parameters. Since the actual shape of the glacial lake surface is irregular, rather than the normal elliptic surface we used in the models, it was crucial to determine how the depth contours move inward based on the actual shape.

We tested two hypotheses. First, utilizing the lakeshore line to continually create buffers inward might depict the depth contours because the depth contours near the lakeshore were the consequence of ongoing indentation of the actual glacial lake surface outline inward. Second, at the 1/4 semi-long axis of the standard elliptic surface, the depth contours would become progressively blurred as the inward indentation continues, thus subsequently using the standard elliptic surface to start the inward indentation (Fig. 5). Importantly, these assumptions were supported by observations of hundreds of glacial lake bathymetric distribution cases worldwide. Some similarities exist between the bathymetric contours and the lakeshore shape, suggesting that the area near the lakeshore is possibly impacted by the slopes around the lake and/or other material sources. There are two explanations for this phenomenon: either the glacial lakes were continuously filled with exogenous debris and rocks, or the initial lake water level had risen and flooded part of the original slopes.

217   The 1/4 semi–long axis is the ending position where the glacial lake is not impacted by exogenous materials, as

218   determined by our understanding of those SCMs. Most of the glacial lake SCMs were located closer to the cone,

219   structured by the straight side of the hemisphere and the upward-opening parabolic side. It is inferred that the initial

220   deepening of the glacial lake is not particularly large from the outer line to the center (compared to the semi–ellipsoid),

221   indicating that exogenous materials are likely to have impacted it. This situation is better understood when the lake

222   SCM is a cone structured by the rightward-opening parabolic side. Therefore, we hypothesized an extreme

223   circumstance in which a glacial lake starts to be significantly influenced by the lake's surroundings' topography. In

224   this case, the slope of the standard rightward-opening parabolic curve is smaller than the slope of the standard straight

225   line and closer to the ideal deepening state of the lake basin when it is larger. This equal slope point is located at the

226   1/4 semi-long axis and represents half of the maximum water depth.
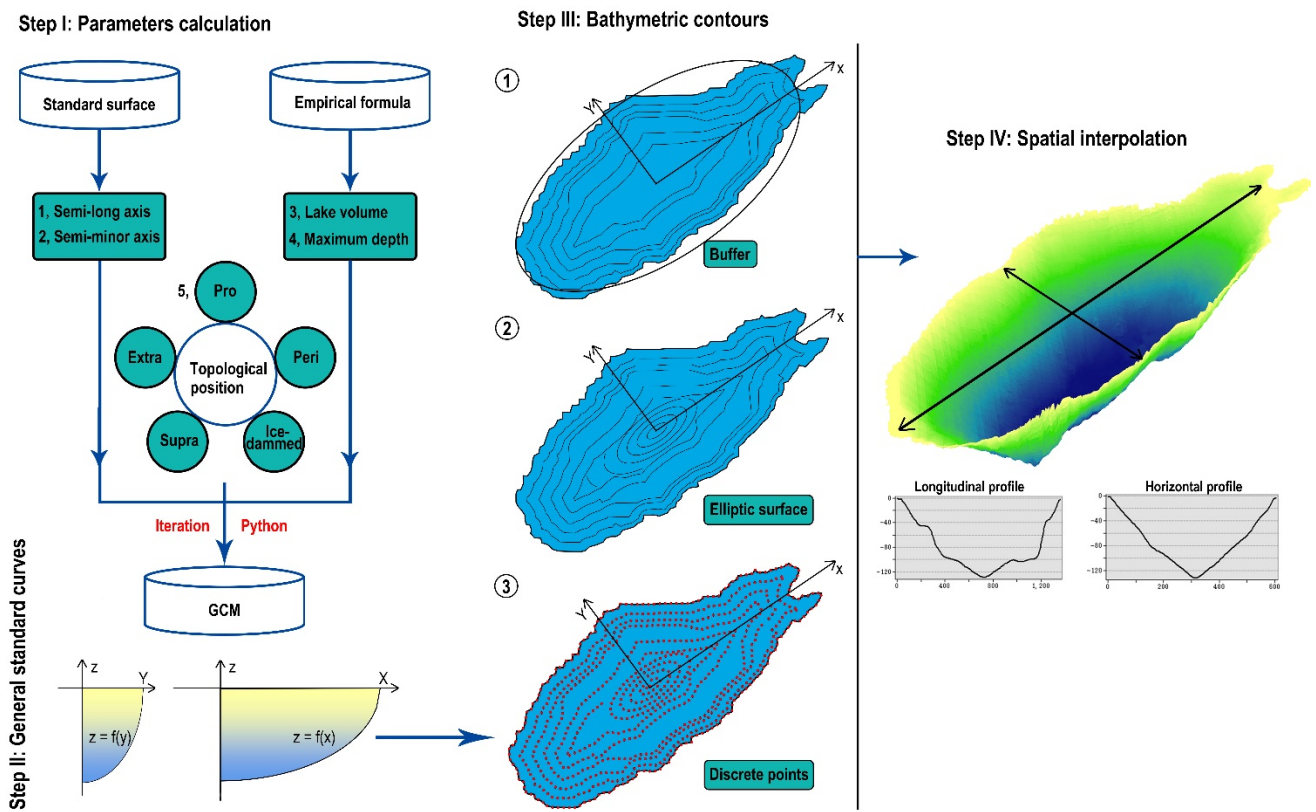
228   **Figure 5.** The procedure illustrates the parameter calculation of GCMs and processes of creating buffers inward. The water depths on

229   the axes were calculated using the standard curves corresponding to the X and Y axes.

## 2.6   Sites for exhibiting and validating results

231   Six sets of bathymetry data were collected for the typical glacial lakes in the Himalayas and Nyainqentanglha

232   (Fig. 6). Among them, Jialongco, Cirenmaco, Poiqu NO.1, and Maqiongco were classified as periglacial lakes, while

the Longbasaba Lake and Dasuopuco were classified as proglacial lakes. Although it would be desirable to evaluate the performance of our conceptual models across different types, sizes, and geographic locations of glacial lakes, we were limited by the available observational data and could only conduct these examinations in the Third Pole region, focusing on proglacial and periglacial lake types. The topological position, total volume, maximum water depth, and semi-long/minor axis of the standard lake surface were crucial parameters in glacial lake bathymetric distribution modeling (Table 2). The six glacial lake bathymetric distributions were simulated according to the lake sizes in the survey year and eventually compared with the measured points of water depths and the overall parameters (total volume and mean water depth) to verify the feasibility and accuracy of our modeling method.

Table 2. The crucial modeling parameters of the six selected glacial lakes.

Name	Lat°	Lon°	Region	Topological position	Survey year	Area (km²)	Volume (10⁶ m³)	Mean water depth (m)	Maximum water depth (m)	Semi-long axis (m)	Semi-minor axis (m)
Jialongco	28.21	85.85	Central Himalaya	periglacial	2020	0.61	37.5	58.2	133	757	314
Cirenmaco	28.07	86.07	Central Himalaya	periglacial	2012	0.33	18.0	55	115	549	185
Poiqu NO.1	28.14	85.92	Central Himalaya	periglacial	2021	0.11	2.7	25.5	75.1	242	129
Maqiongco	30.49	93.36	Nyainqentanglha	periglacial	2021	0.23	3.2	15	33.5	493	168
Longbasaba Lake	27.95	88.08	Eastern Himalaya	proglacial	2009	1.17	64.0	48	102	1949	319
Dasuopuco	28.44	85.78	Central Himalaya	proglacial	2021	0.55	0.55	33.8	93	1362	247
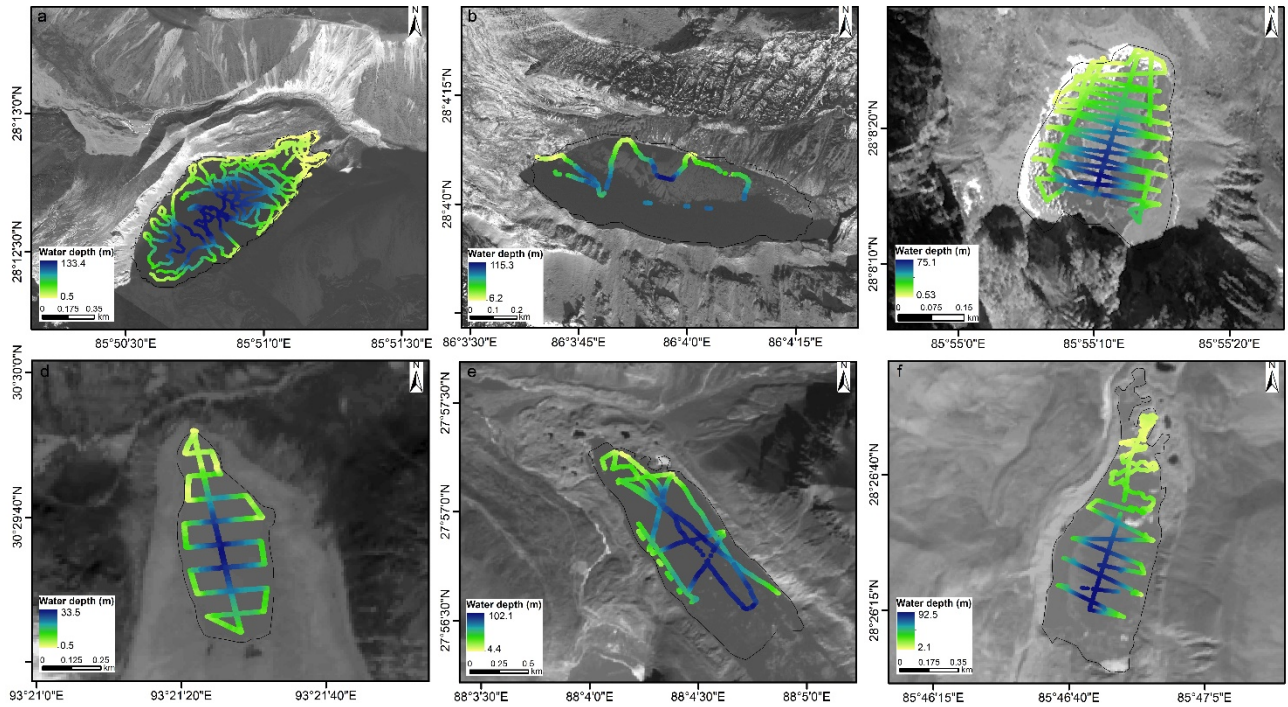
Figure 6. The water depth observed along the bathymetric routes for (a) Jialongco, (b) Cirenmaco, (c) Poiqu NO.1, (d) Maqiongco, (e)

245   Longbasaba Lake, and (f) Dasuopuco.

246

3   Results

248   We present the SCMs for each type of glacial lake and demonstrate a procedure to identify the most compatible

249   GCM for a specific glacial lake by equalizing the volume of both. To our knowledge, this is the first model to simulate

250   the bathymetric distribution of glacial lakes at present. The results reveal that the proglacial and periglacial lakes

251   exhibit greater depths as their SCMs are closer to the hemisphere structured by the upward-opening parabolic side.

252   Conversely, the SCMs of the extraglacial and supraglacial lakes are closer to the cone structured by the straight side,

253   indicating relatively shallower depths. As the ice-dammed lake, their V–A fitting curve is more similar to the V–A

254   curve of the triangular cone (Fig. 4). Hence, we recommend that the bathymetric distribution modeling for ice-

255   dammed lakes proceeds directly using the standard triangular cone.

256   We determined the optimal GCMs for the six exhibited glacial lakes. Following bathymetric distribution

257   modeling results, the total volume of Jialongco was calculated to be 33.1×10^6 m^3 (with a relative error of -11.7%)

258   with a mean water depth of 54.6 m (-8.1%). Its GCM was closer to the cone structured by the straight side (Fig. 7a).

259   The computed total volume and mean depth of Cirenmaco were 17.2×10^6 m^3 (-4.4%) and 51.7 m (-6.9%),

260   respectively. The Cirenmaco GCM had similarities with the hemisphere structured by the upward-opening parabolic

261   side (Fig. 7b), meaning a more significant inward deepening rate than Jialongco. The relatively small-sized Poiqu

262   NO.1 and Maqiongco had total volumes of 2.9×10^6 m^3 (7.4\%) and 3×10^6 m^3 (-6.3\%), and mean water depths of 27.3

263   m (7.1\%) and 12.8 m (-14.7\%), respectively. Their optimal GCMs showed similarities with Jialongco (Fig, 7c, d).

264   The proglacial lake, Longbasaba, was estimated to have a total volume of 71.4×10^6 m^3 (11.5\%) and a mean depth of

265   61.1 m (22.2\%). Its GCM was more resemblant to the semi-ellipsoid (Fig. 8a). Dasuopuco had the smallest relative

266   error in the total volume (0.2\%) and mean water depth (-1.8\%) (Fig. 8b). Overall, approximately $\pm 10\%$ volume

267   uncertainty was estimated in the process of nesting the general conceptual models to the actual glacial lake shapes.

268   The disparity between the area of the assumed standard ellipse surface and the actual lake surface, as well as the

269   deviation of the deepest water location, likely caused the majority of the inaccuracy. The initial settings of glacial

270   lake conceptual models and the algorithm's applicability were confirmed by comparison with the measured and

271   estimated individual water depths. Between the estimated and measured water depths along the bathymetric routes,

272   the average deviation, mean absolute deviation, and root mean square error for the six glacial lakes all described good

273   consistency. Neither near the lakeshore nor the lake center do the estimates show intolerable dispersions.

274
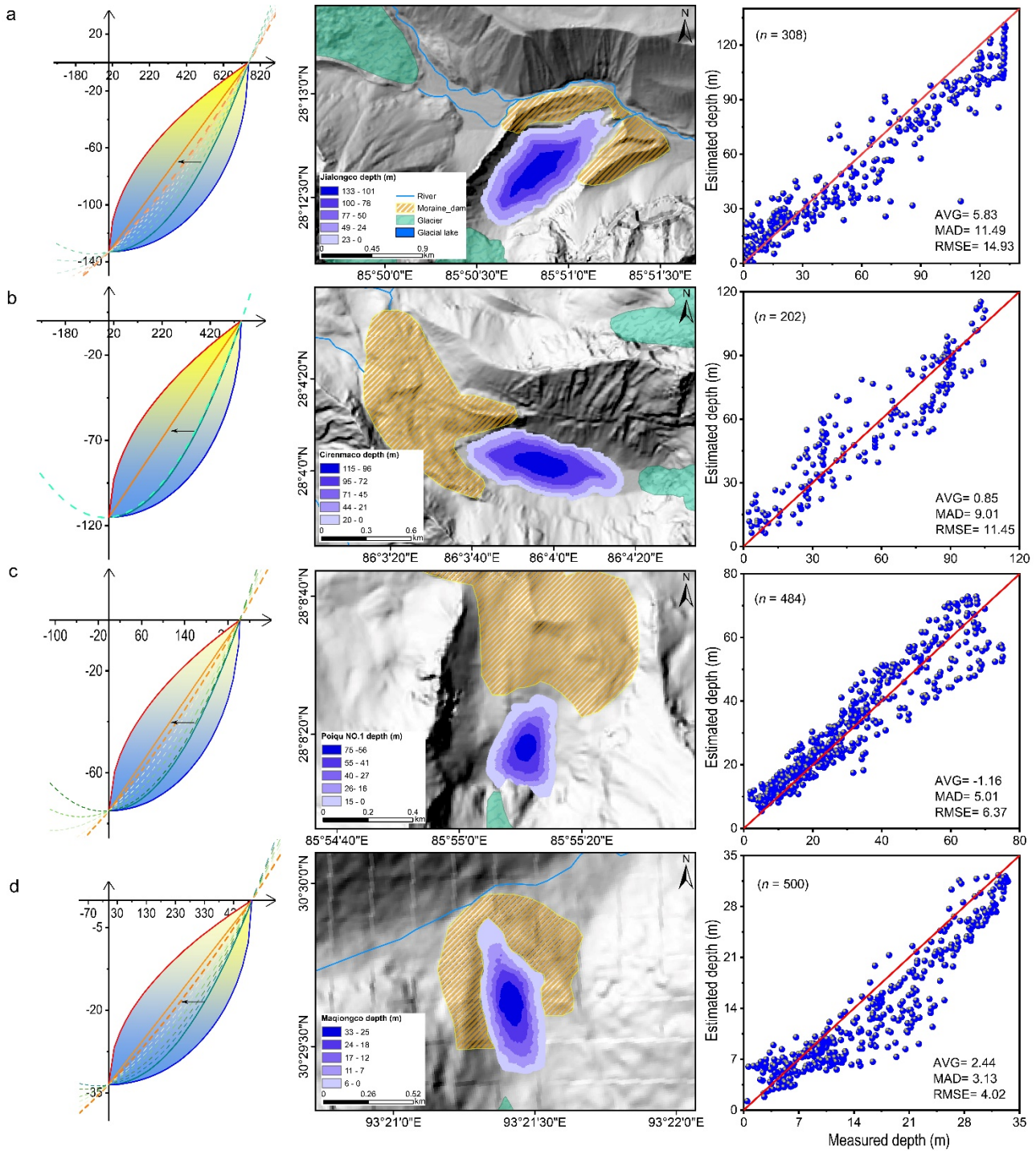
Figure 7. Modeled glacial lake bathymetric distributions of the four selected periglacial lakes. (a) Jialongco, (b) Cirenmaco, (c) Poiqu NO.1, and (d) Maqiongco. The average deviation (AVG), mean absolute deviation (MAD), and root mean square error (RMSE) were selected to depict the consistency between the simulated and measured individual water depths along the boat routes. The movements of the general curves from one standard curve to another are also indicated.

14
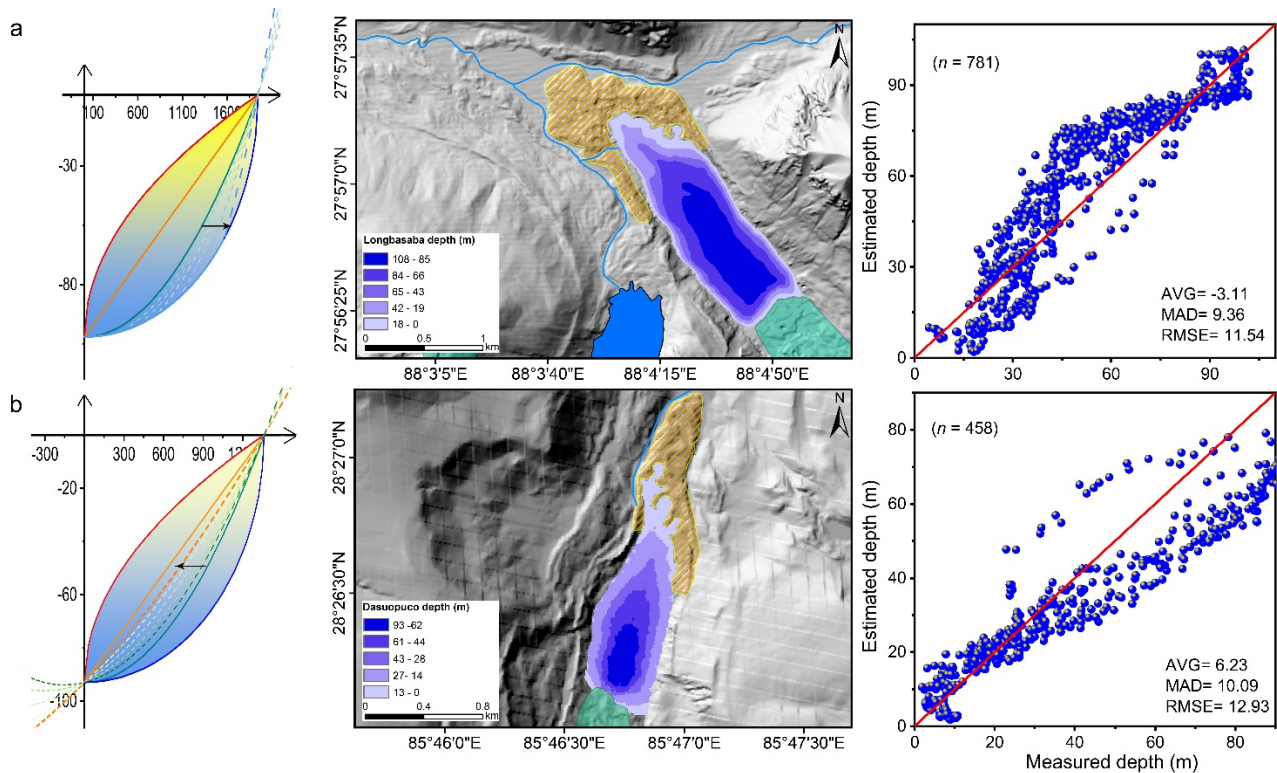
Figure 8. Modeled glacial lake bathymetric distributions of the two selected proglacial lakes. (a) Longbasaba Lake, and (b) Dasuopuco. The average deviation (AVG), mean absolute deviation (MAD), and root mean square error (RMSE) were selected to depict the consistency between the simulated and measured individual water depths along the boat routes. The movements of the general curves from one standard curve to another are also indicated.

4 Discussion

4.1 Glacial lake basin evolution

Understanding the glacial lake evolution can help comprehend these idealized geometric shapes in theory. Most moraine- or bedrock-dammed lakes develop in depressions exposed by diminishing glaciers. The supraglacial lakes exist at the glacier snout, eventually facilitating the formation of proglacial and periglacial lakes (Carrivick and Tweed, 2013; Mertes et al., 2017). As the six glacial lakes illustrated, our hypotheses explained the different rates of inward deepening owing to the influence of exogenous materials. The glacier bedrock has been eroded and nudged during historical ice flowing, posing the excavation and growth of glacial lake basins.

Contemporary glaciers often have a certain thickness of debris at the snout. For example, approximately 1 m of debris was observed at the snout of the Urumqi Glacier No. 1, China (Echelmeyer et al., 1987) as the result of glacial

erosion. The specific sites of continual eroding and nudging spawn overdeepenings and are considered potential glacial lakes (Linsbauer et al., 2016). Since the glacier velocity in the middle part is often larger than that of both sides, the erosion is stronger in the central line of the initial overdeepening. As glacier flowing continues, the shape of the overdeepening finally reaches equilibrium and is similar to a hemisphere, which is the GCM of the lake basin we assumed. After the overdeepenings are exposed, they can be filled by meltwater to form glacial lakes while also receiving material deposition, resulting in a gradual transition of the idealized geometric basin from a hemisphere to a cone. This conjecture can be inferred from the studies of overdeepenings on glacial beds, whereby the volume and surface area of these potential glacial lakes are also in accordance with the power-law relationship (Zhang et al., 2022).

4.2 Applicability of the conceptual model

Our modeling theory is based on the observations of glacial lake bathymetric distribution characteristics worldwide, revealing a geometrical approximation law for glacial lake bathymetry. However, it is strictly limited by several constraints. Firstly, the designed conceptual model is more suitable for those glacial lakes with typically lengthy and elliptical-like shapes, and may be less applicable to very irregularly shaped glacial lakes, such as the ice-marginal and thermokarst lakes in the Greenland and Alaska region (Field et al., 2021; Coulombe et al., 2022). Secondly, the designed conceptual model is also more suitable for those glacial lakes with a cirque-valley glacier or a small/medium sized valley glacier flowing along a straight valley, ensuring idealized formation conditions for the glacial lake basin with minimal erosion and deposition from tributaries. Although the simulated results were only validated in the periglacial and proglacial lakes of the Himalayas and Nyainqentanglha due to limited observation data, the comparison results of the measured and modeled depth values at different locations of the six glacial lakes demonstrates the rationality and reliability of our conceptual models. Further validation is needed to assess the applicability of our conceptual model across different lake types on a global scale. There is a significant limitation in the availability of glacial lake bathymetric distribution data, with most studies only providing key parameters such as total volume, maximum depth, and mean depth. Moreover, due to the challenges of field investigations, measurements of glacial lakes have predominantly focused on larger, hazardous, or particularly interesting peri- and proglacial lakes. This makes us unable to find any available bathymetric distribution data for extraglacial, supraglacial, and ice-dammed lakes, preventing validation of our conceptual model for these lake types.

In addition to the subjective and objective errors made during the modeling phase, there are several systematic

323 defects in the algorithm itself: (1) The total volume and maximum water depth are calculated using empirical

324 equations, which may lead to significant deviations when modeling the bathymetric distribution of an arbitrarily

325 selected glacial lake. Particularly, the curves of D–A are not robust, with many discrete points appearing (Fig. 2). (2)

326 The estimated depth contours converge inward using the lake shoreline buffers first, followed by the elliptical

327 surfaces. This process may effectively simulate the connections between a bathymetric distribution and glacial lake

328 morphology. However, it is not essential. If the elliptical indentations are always inward relative to the elliptical

329 surface, the modeling accuracy is also not affected significantly in theory. (3) The deepest sites of proglacial lakes

330 have been considered to be near the glacier-lake interface. The developing proglacial lakes, however, are complex.

331 Their deepest sites are constantly located near the glacier terminus before the deepest site of overdeepening is exposed

332 (Fig. 9a), which is in accordance with our hypothesis. With the deepest sites developing more fully, they gradually

333 shift toward the lake center. Our algorithm has not addressed these changes. In the future, the conceptual model will

334 require parameter optimization through learning with a number of measured bathymetry data. Furthermore, the

335 present version of our algorithm relies on simple programming and semi-automated geospatial analysis tools

336 processing. We will further develop this conceptual model to create an interface that can automatically process and

337 reduce subjective errors.

338 ## 4.3   Rationality of empirical V-A equations

339   Currently, many studies have attempted to fit V-A equations with regional or global applicability for various

340 types of glacial lakes (Cook et al., 2015; Qi et al., 2022). The most common classification method for glacial lakes is

341 based on dam materials, such as moraine-dammed, bedrock-dammed, and landslide-dammed. However, this study

342 reveals that the different types of glacial lakes have different ideal basin shapes that may be unfavorable to most

343 already formed V-A empirical formulations, although some have high R^2 values (Table 1). For instance, most of the

344 proglacial and periglacial lakes is generally dammed by moraine, involving in many fitting works of V-A relationships.

345 Unreasonably, the incompletely developed basins of proglacial lakes and the fully developed basins of periglacial

346 lakes are often described by same empirical formulas (Fig. 9a), disregarding the distinct basin development stages

347 between them. This aspect has overlooked in the previous studies. In our fitted curves of V-A relationships for various

348 types of glacial lakes (Fig. 4), the V-A relationship for proglacial lakes is robust, indicating possible global

349 applicability. However, the V-A relationships for periglacial and extraglacial lakes exhibit many outliers, suggesting

350 a strong influence from exogenous materials filling in these lakes based on our hypothesis. The V-A relationships of

351 these glacial lakes decoupled with their glaciers at least require parameters related to the glacier characteristics and

352   time of detachment for further description.

353   There is no single classification method can adequately capture the refined characteristics of glacial lakes. Even

354   lakes classified as the same type may differ in terms of parent glaciers, bedrock properties, or dam materials. In the

355   modeling of glacial lake bathymetric distribution, accurately estimating the total volume and maximum water depth

356   of glacial lakes is crucial. Therefore, future studies should not only focus on whether the empirical formula is

357   generalizability or global applicability, but also develop more detailed classification criteria for glacial lakes,

358   comprehensively considering dam materials, topological positions, glacier properties, area intervals, geographic

359   location, and other relevant factors. This will facilitate a well-fitting of regional empirical relationships of V-A and

360   D-A for various types of glacial lakes, thereby reducing the dispersion between data points.
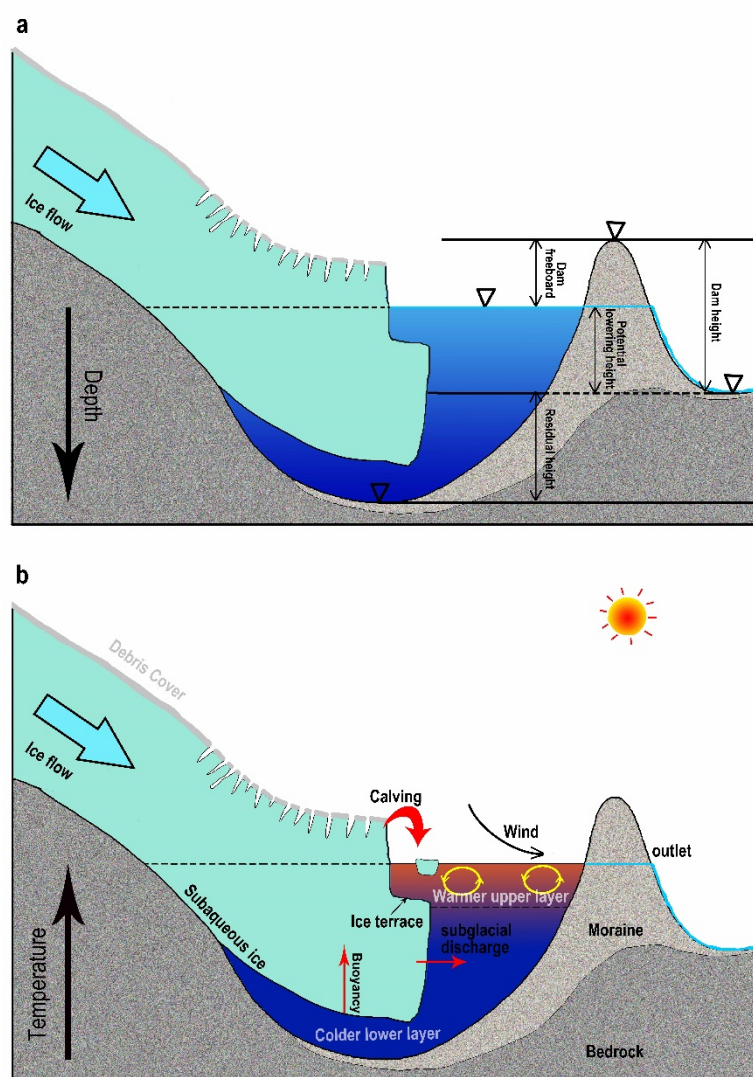
361

362   **Figure 9.** The schematic diagrams illustrate (a) the potential maximum lowering height of the glacial lake water level after drainage and

363   (b) the interactions between the parent glacier and its terminating lake.

18

4.4 Applications in GLOF modeling

The conceptual model has been proposed in this study, one such application is in GLOF modeling. The results make two significant contributions to future GLOF modeling: (i) accurately estimate the maximum potential outburst water volume of a glacial lake by combining lake surface elevation, dam bottom elevation, and the optimal GCM; (ii) facilitate coupling between the various GLOF processes in modeling (trigger–displacement wave–dam breach–flood propagation). Many recent studies have documented reconstructing the historical GLOFs and simulating the future GLOFs from high outburst potential glacial lakes (Allen et al., 2015; Anacona et al., 2015b; Erokhin et al., 2017; Kougkoulos et al., 2018). The modeling precision is expected to improve significantly.

On the one hand, most prior studies replaced the potential maximum outburst volume with the total water volume because of the limitations of glacial lake bathymetric investigations (Zhang et al., 2021). Although this could present a maximized risk assessment, an inflated downstream exposure might raise excessive concerns among the authorities and the public regarding inadequate prevention and mitigation measures (Emmer et al., 2022b). As long as the dam's lowest elevation exceeds that of the glacial lake (potential lowering height is less than the maximum water depth), it could result in incomplete drainage (Fig. 9a). On the other hand, due to the complicated phase transition in the chain process of GLOFs, a segmented simulation has been generally conducted. For instance, Rapid Mass Movement Simulation (RAMMS) can be used to simulate the impact of ice avalanches or landslides on glacial lakes (Frey et al. 2018; Sattar et al. 2021; Duan et al., 2023), and hydrological algorithms are used to calculate the displacement wave (Heller et al. 2009; Evers et al. 2019). Modeling software like IBER, HEC-RAS, or FLO-2D are employed to simulate downstream flood propagation (Alho and Aaltonen, 2008; Osti and Egashira, 2009; Schneider et al., 2014; Somos-Valenzuela et al., 2015; Maurer et al., 2020; Nie et al. 2020).

In contrast to a holistic simulation, such a segmented simulation approach undoubtedly causes poor articulation and increased uncertainty in different processes. With the recent scientific developments, a newly developed three-phase flow model, r.avaflow (Mergili et al., 2017), started to be used to simulate GLOF propagations (Mergili et al., 2018, 2020; Sattar et al., 2023) and can realize the whole hazard cascade modeling with a high performance (Zheng et al., 2021). Our study can provide much-needed glacial lake bathymetry data for such modeling to calculate the displacement wave in the lake surface and the water release process during dam erosion.

4.5 Potential developments of numerical or physical models

The standardized glacial lake basin can facilitate other future model development related to glacial lakes and

improve knowledge of how the proglacial lakes and lake-terminating glaciers interact. Carrivick et al. (2020) discussed six major challenges in constructing a numerical model of interactions between proglacial lakes and glaciers, which include the imperative for glacial lake bathymetry. The standardized shape implicates the design of the model's basic architecture.

Compared with the somewhat realistic glacier bed topography within the overdeepenings revealed by Ice Thickness Models, a standardized lake basin provides an alternative scheme. For a specific proglacial lake, its water level, water temperature, in/outflow, internal circulation, and interface with the glacier vary with glacier-lake dynamics and time, which are very complex processes (Sugiyama et al., 2016; Sutherland et al., 2020). Deep and large proglacial lakes are prone to water stratification due to warmer upper layers and colder lower layers of water because these freshwater terminating lakes currently have no evidence of active internal circulation (Haresign and Warren, 2005; Boyce et al., 2007). This stratification induces the subaqueous ice differential melting and ice terrace formation (Fig. 9b), impacting the glacier terminal calving regimes (Sugiyama et al., 2019; Mallalieu et al., 2020). On the other hand, the dynamic characteristics of glacier snout, such as bed friction, longitudinal stress, and ice flow velocity, vary distinctively due to the presence of terminating lakes (Sugiyama et al., 2011; Liu et al., 2020). The knowledge and understanding of glacial lakes formation and evolution changes continually. The ultimate goal is to present these processes via computer numerical simulations. Yet, the idealized lake basin can facilitate calculating the mass and energy transport at the interface.

5 Conclusion

This study was conducted in response to a circumstance that field investigation was the only approach to obtain glacial lake bathymetry. The relationships of volume–area and maximum water depth–area of glacial lakes were reanalyzed via an inventory of the global glacial lake bathymetry data we compiled. The obtained curves were matched with a power-law relationship. Thus, the types of hemispheres or cones were determined as the conceptual models (idealized geometric shapes) of glacial lakes. The standard lake surface was assumed to be an ellipse.

Nine standard conceptual models were identified. The SCMs for the supraglacial, periglacial, and extraglacial lakes are the hemisphere structured by the elliptical side; the hemisphere structured by the upward-opening parabolic side; the cone structured by the straight side; and the cone structured by the rightward-opening parabolic side. The SCMs for the proglacial lakes were determined to be half of the aforementioned four SCMs. Two SCMs were

420   considered for the ice-dammed lakes: the semi–cone structured by the straight side and the triangular cone. To depict

421   the volume between the two SCMs, a general conceptual model was defined to represent the transition from one

422   SCM to another.

423   Several hypotheses are important in our algorithm to nest the actual glacial lake shapes from idealized

424   conceptual models and interpolate glacial lake bathymetric distribution. First, the supraglacial, periglacial, and

425   extraglacial lakes' deepest sites were assumed to be in the lake center, whereas the proglacial lakes and ice-dammed

426   lakes' deepest sites were near the glacier-lake interface. Second, the effects of exogenous materials and boundary

427   conditions were used to explain the different rates of inward deepening of glacial lakes. Six glacial lakes with

428   measured bathymetry data were selected in the Third Pole region for comparison with the simulated bathymetric

429   distributions. The results demonstrated good accuracy and applicability of our conceptual models in estimating lake

430   bathymetry. Relatively high consistency was shown in the point-to-point comparisons of the measured and simulated

431   water depths. This study constructed the glacial lake bathymetric distribution model which is very rewarding for

432   comprehending the evolution of glacial lakes. Moreover, the quality of GLOF modeling and risk assessment is also

433   enhanced by our outlined general conceptual model. These standardized lake basins implicate the design of the

434   model's basic architecture, which can potentially promote the development of future numerical or physical models

435   of glacial lakes.

436

References

Aggarwal, S., Rai, S. C., Thakur, P. K., and Emmer, A.: Inventory and recently increasing GLOF susceptibility of glacial lakes in Sikkim, Eastern Himalaya, Geomorphology, 295, 39–54, http://dx.doi.org/10.1016/j.geomorph.2017.06.014, 2017.

Alho, P., and Aaltonen, J.: Comparing a 1D hydraulic model with a 2D hydraulic model for the simulation of extreme glacial outburst floods, Hydrol. Process, 22, 1537–1547. http://dx.doi.org/10.1002/hyp.6692, 2018.

Allen, S. K., Rastner, P., Arora, M., Huggel, C., and Stoffel, M. (2016). Lake outburst and debris flow disaster at Kedarnath, June 2013: hydrometeorological triggering and topographic predisposition, Landslides, 13, 1479–1491, http://dx.doi.org/10.1007/s10346-015-0584-3, 2015.

Anacona, P. I., Mackintosh, A., Norton, K. P.: Hazardous processes and events from glacier and permafrost areas: lessons from the Chilean and Argentinean Andes, Earth Surf. Process Landf., 40, 2–21, http://dx.doi.org/10.1002/esp.3524, 2015a.

Anacona, P. I., Mackintosh, A., Norton, K.: Reconstruction of a glacial lake outburst flood (GLOF) in the Engano Valley, Chilean Patagonia: Lessons for GLOF risk management, Sci. Total Environ., 527–528, 1–11, http://dx.doi.org/10.1016/j.scitotenv.2015.04.096, 2015b.

Bolch, T., Buchroithner, M. F., Peters, J., Pradhan, B., Buchroithner, M., and Blagoveshchensky, V.: Identification of glacier motion and potentially dangerous glacial lakes in the mt. Everest region/Nepal using spaceborne imagery, Nat. Hazard Earth Syst., 8, 1329–1340, http://dx.doi.org/10.1007/s11069-011-9860-2, 2011.

Boyce, E. S., Motyka, R. J., and Truffer, M.: Flotation and retreat of a lake-calving terminus, Mendenhall Glacier, southeast Alaska, USA, J. of Glaciol., 53, 211–224, http://dx.doi.org/10.3189/172756507782202928, 2007.

Carrivick, J. L., and Tweed, F. S.: Proglacial lakes: character, behaviour and geological importance, Quat. Sci. Rev.,78, 34–52, http://dx.doi.org/10.1016/j.quascirev.2013.07.028, 2013.

Carrivick, J. L., and Tweed, F. S.: A global assessment of the societal impacts of glacier outburst floods, Glob. Planet. Change, 144, 1–16, http://dx.doi.org/10.1016/j.gloplacha.2016.07.001, 2016.

Carrivick, J. L., Tweed, F. S., Sutherland, J. L., and Mallalieu, J.: Toward numerical modeling of interactions between ice-marginal proglacial lakes and glaciers, Front. Earth Sci., 500, https://doi.org/10.3389/feart.2020.577068, 2020.

Cook, S. J., Quincey, D. J.: Estimating the volume of Alpine glacial lakes, Earth Surf.. Dyn, 3, 559–575, http://www.earth-surf-dynam.net/3/559/2015/doi:10.5194/esurf-3-559-2015, 2015.

Coulombe, S., Fortier, D., Bouchard, F., Paquette, M., Charbonneau, S., Lacelle, D., Laurion, I. and Pienitz, R. Contrasted geomorphological and limnological properties of thermokarst lakes formed in buried glacier ice and ice-wedge polygon terrain, Cryosphere, 16, 2837–2857. https://doi.org/10.5194/tc-16-2837-2022, 2022.

Drenkhan, F., Huggel, C., Guardamino, L., and Haeberli, W.: Managing risks and future options from new lakes in the deglaciating Andes of Peru: The example of the Vilcanota-Urubamba basin, Sci. Total Environ., 665, 465–483, https://doi.org/10.1016/j.scitotenv.2019.02.070, 2019.

Duan, H., Yao, X., Zhang, Y., Jin, H., Wang, Q., Du, Z., Hu, J., Wang, B., and Wang, Q.: Lake volume and potential hazards of moraine-

486   dammed glacial lakes–a case study of Bienong Co, southeastern Tibetan Plateau. Cryosphere, 17, 591–616,
487   https://doi.org/10.5194/tc-17-591-2023, 2023.

488   Echelmeyer, K., Wang Z. X.: Direct observation of basal sliding and deformation of basal drift at sub-freezing temperatures, J. Glaciol.,
489   33, 83–98. http://dx.doi.org/10.3189/s0022143000005396, 1987.

490   Emmer, A., and Vilímek, V.: New method for assessing the susceptibility of glacial lakes to outburst floods in the Cordillera Blanca,
491   Peru, Hydrol. Earth Syst. Sci., 18, 3461–3479, http://www.hydrol-earth-syst-sci.net/18/3461/2014/doi:10.5194/hess-18-3461-2014,
492   2014.

493   Emmer, A., Klimeš, J., Mergili, M., Vilímek, V. and Cochachin, A.: 882 lakes of the Cordillera Blanca: An inventory, classification,
494   evolution and assessment of susceptibility to outburst floods, Catena, 147, 269–279, http://dx.doi.org/10.1016/j.catena.2016.07.032,
495   2016.

496   Emmer, A., Allen, S.K., Carey, M., Frey, H., Huggel, C., Korup, O., Mergili, M., Sattar, A., Veh, G., Chen, T.Y., Cook, S.J., Correas-
497   Gonzalez, M., Das, S., Diaz Moreno, A., Drenkhan, F., Fischer, M., Immerzeel, W.W., Izagirre, E., Joshi, R.C., Kougkoulos, I.,
498   Kuyakanon Knapp, R., Li, D., Majeed, U., Matti, S., Moulton, H., Nick, F., Piroton, V., Rashid, I., Reza, M., Ribeiro de Figueiredo,
499   A., Riveros, C., Shrestha, F., Shrestha, M., Steiner, J., Walker-Crawford, N., Wood, J.L. and Yde, J.C. Progress and challenges in
500   glacial lake outburst flood research (2017–2021): a research community perspective, Nat. Hazard Earth Sys. Sci., 22, 3041–3061.
501   https://doi.org/10.5194/nhess-22-3041-2022, 2022a.

502   Emmer, A., Wood, J.L., Cook, S.J., Harrison, S., Wilson, R., Diaz-Moreno, A., Reynolds, J.M., Torres, J.C., Yarleque, C., Mergili, M.,
503   Jara, H.W., Bennett, G., Caballero, A., Glasser, N.F., Melgarejo, E., Riveros, C., Shannon, S., Turpo, E., Tinoco, T., Torres, L.,
504   Garay, D., Villafane, H., Garrido, H., Martinez, C., Apaza, N., Araujo, J. and Poma, C. 160 glacial lake outburst floods (GLOFs)
505   across the Tropical Andes since the Little Ice Age, Global Plane. Change, 208. https://doi.org/10.1016/j.gloplacha.2021.103722,
506   2022b.

507   Erokhin, S. A., Zaginaev, V. V., Meleshko, A. A., Ruiz-Villanueva, V., Petrakov, D. A., Chernomorets, S. S., Viskhadzhieva, K. S.,
508   Tutubalina, O. V., and Stoffel, M.: Debris flows triggered from non-stationary glacier lake outbursts: the case of the Teztor Lake
509   complex (Northern Tian Shan, Kyrgyzstan), Landslides, 15, 83–98, http://dx.doi.org/10.1007/s10346-017-0862-3, 2018.

510   Evans, S. G.: The maximum discharge of outburst floods caused by the breaching of man-made and natural dams, Can. Geotech. J.,
511   23(3), 385–387, http://dx.doi.org/10.1139/t87-062, 1986.

512   Evers F. M., Heller, V., Fuchs, H., Hager, W. H., and Boes, R. M.: Landslide-generated Impulse Waves in Reservoirs: Basics and
513   Computation, VAW-Mitteilungen, 254, 2019.

514   Falatkova, K., Šobr, M., Neureiter, A., Schöner, W., Janský, B., Häusler, H., Engel, Z., and Beneš, V.: Development of proglacial lakes
515   and evaluation of related outburst susceptibility at the Adygine ice-debris complex, northern Tien Shan, Earth Surf. Dyn., 7, 301–
516   320, https://doi.org/10.5194/esurf-7-301-2019, 2019.

517   Field, H. R., Armstrong, W. H. and Huss, M.: Gulf of Alaska ice-marginal lake area change over the Landsat record and potential physical
518   controls, Cryosphere, 15, 3255–3278. https://doi.org/10.5194/tc-15-3255-2021, 2021.

519   Frey, H., Huggel, C., Chisolm, R. E., Baer, P., McArdell, B., Cochachin, A., and Portocarrero, C.: Multi-source glacial lake outburst
520   flood hazard assessment and mapping for Huaraz, Cordillera Blanca, Peru, Front. Earth Sci., 6, 210.
521   https://doi.org/10.3389/feart.2018.00210, 2018.

522   Fujita, K., Sakai, A., Takenaka, S., Nuimura, T., Surazakov, A. B., Sawagaki, T., and Yamanokuchi, T.: Potential flood volume of
523   Himalayan glacial lakes, Nat. Hazard Earth Syst. Sci., 13, 1827–1839, http://www.nat-hazards-earth-syst-
524   sci.net/13/1827/2013/doi:10.5194/nhess-13-1827-2013, 2013.

525   Gu, C., Li, S., Liu, M., Hu, K., and Wang, P.: Monitoring Glacier Lake Outburst Flood (GLOF) of Lake Merzbacher Using Dense Chinese
526   High-Resolution Satellite Images. Remote Sens., 15, https://doi.org/10.3390/rs15071941, 2023.

527   Haresign, E., and Warren, C. R.: Melt rates at calving termini: a study at Glaciar León, Chilean Patagonia, Geological Society, London,
528   Special Publications, 242, 99–109, http://dx.doi.org/10.1144/GSL.SP.2005.242.01.09, 2005.

529   Heller, V., Hager, W. H., Minor, H. E.: Landslide Generated Impulse Waves in Reservoirs, Zurich: Mitteilungen Versuchsanstalt für

Wasserbau, Hydrologie und Glaziologie (VAW), ETH Zürich, 2019.

Huggel, C., Kääb, A., Haeberli, W., Haeberli, W., Teysseire, P., and Paul, F.: Remote sensing based assessment of hazards from glacier lake outbursts: a case study in the Swiss Alps, Can. Geotech. J., 39, 316–330, http://dx.doi.org/10.1139/t01-099, 2002.

Hugonnet, R., McNabb, R., Berthier, E., Menounos, B., Nuth, C., Girod, L., Farinotti, D., Huss, M., Dussaillant, I., Brun, F., and Kääb, A.: Accelerated global glacier mass loss in the early twenty-first century, Nature, 592, 726–731, https://doi.org/10.1038/s41586-021-03436-z, 2021.

Kapitsa, V., Shahgedanova, M., Machguth, H., Severskiy, I., and Medeu, A.: Assessment of evolution and risks of glacier lake outbursts in the Djungarskiy Alatau, Central Asia, using Landsat imagery and glacier bed topography modelling, Nat. Hazard Earth Syst. Sci., 17, 1837–1856, https://doi.org/10.5194/nhess-17-1837-2017, 2017.

Khanal, N. R., Hu, J. M., and Mool, P.: Glacial lake outburst flood risk in the Poiqu/Bhote Koshi/Sun Koshi river basin in the Central Himalayas, Mt. Res. Dev., 35, 351–364, http://dx.doi.org/10.1659/MRD-JOURNAL-D-15-00009, 2015.

Kougkoulos, I., Cook, S. J., Edwards, L. A., Clarke, L. J., Symeonakis, E., Dortch, J. M., and Nesbitt, K.: Modelling glacial lake outburst flood impacts in the Bolivian Andes, Nat. Hazard, 94, 1415–1438, https://doi.org/10.1007/s11069-018-3486-6, 2018.

Li, D., Shangguan, D. H, Wang, X., Ding, Y. J., Su, P. C., Liu, R. L., and Wang, M. X.: Expansion and hazard risk assessment of glacial lake Jialong Co in the central Himalayas by using an unmanned surface vessel and remote sensing, Sci. Total Environ., 784, https://doi.org/10.1016/j.scitotenv.2021.147249, 2021.

Linsbauer, A., Frey, H., Haeberli, W., Machguth, H., Azam, M. F., and Allen, S.: Modelling glacier-bed overdeepenings and possible future lakes for the glaciers in the Himalaya—Karakoram region, Ann. Glaciol., 57, 119–130, http://dx.doi.org/10.3189/2016AoG71A627, 2016.

Liu, Q., Mayer, C., Wang, X., Nie, Y., Wu, K. P., Wei, J. F., and Liu, S. Y.: Interannual flow dynamics driven by frontal retreat of a lake-terminating glacier in the Chinese Central Himalaya, Earth Planet. Sci. Lett., 546, 116450, https://doi.org/10.1016/j.epsl.2020.116450, 2020.

Lliboutry, L., Arnao, B. M., Pautre, A., and Schneider, B.: Glaciological problems set by the control of dangerous lakes in Cordillera Blanca, Peru. I. Historical failures of morainic dams, their causes and prevention, J. Glaciol., 18, 239–254, http://dx.doi.org/10.1017/S002214300002133X, 1977.

Loriaux, T., Casassa, G.: Evolution of glacial lakes from the Northern Patagonia Icefield and terrestrial water storage in a sea-level rise context, Glob. Planet. Change, 102, 33–40, http://dx.doi.org/10.1016/j.gloplacha.2012.12.012, 2013.

Lützow, N., Veh, G. and Korup, O. A global database of historic glacier lake outburst floods, Earth Sys. Sci. Data, (in discussion). http://dx.doi.org/10.5194/essd-2022-449, 2023.

Ma. J. S., Song. C. Q., Wang, Y. J.: Spatially and Temporally Resolved Monitoring of Glacial Lake Changes in Alps During the Recent Two Decades, Front. Earth Sci., 9, https://doi.org/10.3389/feart.2021.723386, 2021.

Mallalieu, J., Carrivick, J. L., Quincey, D. J., and Smith, M. W.: Calving seasonality associated with melt-undercutting and lake ice cover, Geophys. Res. Let., 47, e2019GL086561, https://doi.org/10.1029/2019GL086561, 2020.

Maurer, J. M., Schaefer, J. M., Russell, J. B., Rupper, S., Wangdi, N., Putnam, A. E., and Young, N.: Seismic observations, numerical modeling, and geomorphic analysis of a glacier lake outburst flood in the Himalayas, Sci. Adv., 6, eaba3645, http://dx.doi.org/10.1126/sciadv.aba3645, 2020.

Mergili, M., Fischer, J. T., Krenn, J., Pudasaini, S. P.: r. avaflow v1, an advanced open-source computational framework for the propagation and interaction of two-phase mass flows, Geosci. Model Develop., 10, 553–569, http://dx.doi.org/10.5194/gmd-10-553-2017, 2017.

Mergili, M., Emmer, A., Juricova, A., Cochachin, A., Fischer, G. T., Huggel, C., and Pudasaini, S. P.: How well can we simulate complex hydro-geomorphic process chains? The 2012 multi-lake outburst flood in the Santa Cruz Valley (Cordillera Blanca, Peru), Earth Surf. Process. Landf., 431373–1389, http://dx.doi.org/10.1002/esp.4318, 2018.

Mergili M, Pudasaini SP, Emmer A, Fischer, G. T., Cochachin, A., Frey, H.: Reconstruction of the 1941 GLOF process chain at Lake Palcacocha (Cordillera Blanca, Peru), Hydrol. Earth Syst. Sci., 24, 93–114, https://doi.org/10.5194/hess-24-93-2020, 2020.

Mertes, J. R., Thompson, S. S., Booth, A. D., Gulley, J. D., and Benn, D. I.: A conceptual model of supra-glacial lake formation on debris-covered glaciers based on GPR facies analysis. Earth Surf. Process. Landf., 42, 903–914, http://dx.doi.org/10.1002/esp.4068, 2017.

Miles, E. S., Watson, C. S., Brun, F., Berthier, E., Esteves, M., Quincey, D. J., Miles, K. E., Hubbard, B., and Wagnon, P.: Glacial and geomorphic effects of a supraglacial lake drainage and outburst event, Everest region, Nepal Himalaya, The Cryosphere, 12, 3891–3905, https://doi.org/10.5194/tc-12-3891-2018, 2018.

Minowa, M., Schaefer, M., and Skvarca, P.: Effects of topography on dynamics and mass loss of lake-terminating glaciers in southern Patagonia. J. Glaciol., 1–18, https://doi.org/10.1017/jog.2023.42, 2023.

Muñoz, R, Huggel, C., Frey, H., Cochachin, A., and Haeberli, W.: Glacial lake depth and volume estimation based on a large bathymetric dataset from the Cordillera Blanca, Peru, Earth Surf. Process. Landf., http://dx.doi.org/10.1002/esp.4826, 2020.

Nie, Y., Liu, Q., Wang, J. D., Zhang, Y. L., Sheng, Y. W., and Liu, S. Y.: An inventory of historical glacial lake outburst floods in the Himalayas based on remote sensing observations and geomorphological analysis, Geomorphology, 308, 91–106, https://doi.org/10.1016/j.geomorph.2018.02.002, 2018.

Nie, Y., Liu, W., Liu, Q., Hu, X., and Westoby, M. J.: Reconstructing the Chongbaxia Tsho glacial lake outburst flood in the Eastern Himalaya: Evolution, process and impacts, Geomorphology, 370, 107393, https://doi.org/10.1016/j.geomorph.2020.107393, 2020.

O'Connor, J. E., Hardison III, J. H., Costa, J. E.: Debris Flows from Failures of Neoglacial-Age Moraine Dams in the Three Sisters and Mount Jefferson Wilderness Areas, Oregon, 105 pp, 2001.

Osti, R., and Egashira, S.: Hydrodynamic characteristics of the Tam Pokhari glacial lake outburst flood in the Mt. Everest region, Nepal, Hydrol. Process., 23, 2943–2955, http://dx.doi.org/10.1002/hyp.7405, 2009.

Patel, L. K., Sharma, P., Laluraj, C. M., Thamban, M., Singh, A., and Ravindra, R.: A geospatial analysis of Samudra Tapu and Gepang Gath glacial lakes in the Chandra Basin, Western Himalaya, Nat. Hazard, 86, 1275–1290, https://link.springer.com/article/10.1007/s11069-017-2743-4, 2017.

Petrov, M. A., Sabitov, T. Y., Tomashevskaya, I. G., Glazirin, G. E., Chernomorets, S. S., Savernyuk, E. A., Tutubalina, O. V., Petrakov, D. A., Sokolov, L. S., Dokukin, M. D., Mountrakis, G., Ruiz-Villanueva, V., and Stoffel, M.: Glacial lake inventory and lake outburst potential in Uzbekistan, Sci. Total Environ., 592, 228–242, http://dx.doi.org/10.1016/j.scitotenv.2017.03.068, 2017.

Qi, M. M., Liu, S. Y., Wu, K. P., Zhu, Y., Xie, F. M., Jin, H., Gao, Y. P. and Yao, X. J. Improving the accuracy of glacial lake volume estimation: A case study in the Poiqu basin, central Himalayas, J. Hydrol., 610. https://doi.org/10.1016/j.jhydrol.2022.127973, 2022.

Rick, B., McGrath, D., Armstrong, W. and McCoy, S.W. Dam type and lake location characterize ice-marginal lake area change in Alaska and NW Canada between 1984 and 2019, Cryosphere, 16, 297–314. https://doi.org/10.5194/tc-16-297-2022, 2022.

Richardson, S. D., Reynolds, J. M.: An overview of glacial hazards in the Himalayas, Quat. Int., 65–6, 31–47, http://dx.doi.org/10.1016/S1040-6182(99)00035-X, 2000.

Sakai, A.: Glacial lakes in the Himalayas: a review on formation and expansion processes, Glob. Environ. Res., 16, 23–30, 2012.

Sattar, A., Haritashya, U. K., Kargel, J. S., Leonard, G. J., Shugar, D. H., and Chase, D. V.: Modeling lake outburst and downstream hazard assessment of the Lower Barun Glacial Lake, Nepal Himalaya, J. Hydrol., 598, 126208. https://doi.org/10.1016/j.jhydrol.2021.126208, 2021.

Sattar, A., Allen, S., Mergili, M., Haeberli, W., Frey, H., Kulkarni, A. V., Haritashya, U. K., Huggel, C., Goswami, A., and Ramsankaran, R.: Modeling Potential Glacial Lake Outburst Flood Process Chains and Effects From Artificial Lake-Level Lowering at Gepang Gath Lake, Indian Himalaya. J. Geophy. Res. Earth Surf., 128, https://doi.org/10.1029/2022JF006826, 2023.

Schneider, D., Huggel, C., Cochachin, A., Guillén, S., and García, J.: Mapping hazards from glacier lake outburst floods based on modelling of process cascades at Lake 513, Carhuaz, Peru, Adv. Geosci., 35, 145–155, http://dx.doi.org/10.5194/adgeo-35-145-2014, 2014.

Sharma, R. K., Pradhan, P., Sharma, N. P., and Shrestha, D. G.: Remote sensing and in situ-based assessment of rapidly growing South Lhonak glacial lake in eastern Himalaya, India, Nat. Hazard, 93, 393–409, https://doi.org/10.1007/s11069-018-3305-0, 2018.

Shugar, D. H., Burr, A., Haritashya, U. K., Kargel, J. S., Watson, C. S., Kennedy, M. C., Bevington, A. R., Betts, R. A., Harrison, S., and

Strattman, K.: Rapid worldwide growth of glacial lakes since 1990, Nat. Clim. Change, 10, 939–945, https://doi.org/10.1038/s41558-020-0855-4, 2020.

Singh, H., Varade, D., de Vries, M.V.W., Adhikari, K., Rawat, M., Awasthi, S., Rawat, D.: Assessment of potential present and future glacial lake outburst flood hazard in the Hunza valley: A case study of Shisper and Mochowar glacier, Sci. Total Environ., 868, 161717, https://doi.org/10.1016/j.scitotenv.2023.161717, 2023.

Somos-Valenzuela, M. A., McKinney, D. C., Byers, A. C., Rounce, D. R., Portocarrero, C., and Lamsal, D.: Assessing downstream flood impacts due to a potential GLOF from Imja Tsho in Nepal, Hydrol. Earth Syst. Sci., 19, 1401–1412, http://dx.doi.org/10.5194/hess-19-1401-2015, 2015.

Sugiyama, S., Skvarca, P., Naito, N., Enomoto, H., Tsutaki, S., Tone,K., Marinsek, S., and Aniya, M.: Ice speed of a calving glacier modulated by small fluctuations in basal water pressure, Nat. Geosci., 4, 597–600, http://dx.doi.org/10.1038/ngeo1218, 2011.

Sugiyama, S., Minowa, M., Sakakibara, D., Skvarca, P., Sawagaki, T., Ohashi, Y., Naito, N., and Chikita, K.: Thermal structure of proglacial lakes in Patagonia, J. Geophys. Res.: Earth Surf., 121, 2270–2286, http://dx.doi.org/10.1002/2016JF004084, 2016.

Sugiyama, S., Minowa, M., and Schaefer, M.: Underwater ice terrace observed at the front of Glaciar Grey, a freshwater calving glacier in Patagonia, Geophys. Res. Let., 46, 2602–2609, http://dx.doi.org/10.1029/2018GL081441, 2019.

Sugiyama, S., Minowa, M., Fukamachi, Y., Hata, S., Yamamoto, Y., Sauter, T., Schneider, C., and Schaefer, M.: Subglacial discharge controls seasonal variations in the thermal structure of a glacial lake in Patagonia, Nat. Commun., 12, 1–9, https://doi.org/10.1038/s41467-021-26578-0, 2021.

Sutherland, J. L., Carrivick, J. L., Gandy, N., Shulmeister, J., Quincey, D. J., and Cornford, S. L.: Proglacial lakes control glacier geometry and behavior during recession, Geophys. Res. Let., 47, e2020GL088865, https://doi.org/10.1029/2020GL088865, 2020.

Veh, G., Korup, O., and Walz, A.: Hazard from Himalayan glacier lake outburst floods, PNAS, 117, 907–912, https://www.pnas.org/cgi/doi/10.1073/pnas.1914898117, 2020.

Wang, X., Liu, S. Y., Ding, Y. J., Guo, W. Q., Jiang, Z. L., Lin, J., and Han, Y.: An approach for estimating the breach probabilities of moraine-dammed lakes in the Chinese Himalayas using remote-sensing data, Nat. Hazard Earth Syst. Sci., 12, 3109–3122, http://dx.doi.org/10.5194/nhess-12-3109-2012, 2012.

Wang, X., Guo, X. Y., Yang C. D., Liu, Q. H., Wei, J. F., Zhang, Y., Liu, S. Y., Zhang, Y. L., Jiang, Z. L., and Tang, Z. G.: Glacial lake inventory of high-mountain Asia in 1990 and 2018 derived from Landsat images, Earth Syst. Sci. Data, 12, 2169–2182, https://doi.org/10.5194/essd-12-2169-2020, 2020.

Wang, W. C., Gao, Y., Anacona, P. I., Lei, Y. B., Xiang, Y., Zhang, G. Q., Li, S. H., and Lu, A. X.: Integrated hazard assessment of Cirenmaco glacial lake in Zhangzangbo valley, Central Himalayas, Geomorphology, 306, 292–305, http://dx.doi.org/10.1016/j.geomorph.2015.08.013, 2018.

Watson, C. S., Quincey, D. J., Carrivick, J. L., Smith, M. W., Rowan, A. V., and Richardson, R.: Heterogeneous water storage and thermal regime of supraglacial ponds on debris-covered glaciers, Earth Surf. Process. Landf., 43, 229–241, http://dx.doi.org/10.1002/esp.4236, 2018.

Watson, C. S., Kargel, J. S., Shugar, D. H., Haritashya, U. K., Schiassi, E., and Furfaro, R. Mass Loss From Calving in Himalayan Proglacial Lakes Front. Earth Sci. 7, 342, http://dx.doi.org/10.3389/feart.2019.00342, 2020.

Wei, J., Liu, S., Wang, X., Zhang, Y., Jiang, Z., Wu, K., Zhang, Z., and Zhang, T.: Longbasaba Glacier recession and contribution to its proglacial lake volume between 1988 and 2018. J. Glaciol., 1–12, https://doi.org/10.1017/jog.2020.119, 2021.

Westoby, M. J., Glasser, N. F., Brasington, J., Hambrey, M. J., Quincey, D. J., and Reynolds, J. M.: Modelling outburst floods from moraine-dammed glacial lakes, Earth-Sci. Rev., 134, 137–159, http://dx.doi.org/10.1016/j.earscirev.2014.03.009, 2014.

Wood, J. L., Harrison, S., Wilson, R., Emmer, A., Yarleque, C., Glasser, N. F., Torres, J. C., Caballero, A., Araujo, J., Bennett, G. L., Diaz-Moreno, A., Garay, D., Jara, H., Poma, C., Reynolds, J. M., Riveros, C. A., Romero, E., Shannon, S., Tinoco, T., Turpo, E., and Villafane, H.: Contemporary glacial lakes in the Peruvian Andes, Glob. Planet. Change, 204, 103574, https://doi.org/10.1016/j.gloplacha.2021.103574, 2021.

Yao, T. D., Thompson, L., Yang, W., Yu, W. S., Gao, Y., Guo, X. J., Yang, X. X., Duan, K. Q., Zhao, H. B., Xu, B. Q., Pu, J. C., Lu, A.

X., Xiang, Y., Kalltel, D. B., and Joswiak, D.: Different glacier status with atmospheric circulations in Tibetan Plateau and surroundings, Nat. Clim. Change, 2, 663–667, http://www.nature.com/doifinder/10.1038/nclimate1580, 2012.

Yao, T. D., Xue, Y. K., Chen, D. L., Chen, F. H., Thompson, L., Cui, P., Koike, T., K.-M. Lau, W., Lettenmaier, D., Mosbrugger, V., Zhang, R. H., Xu, B. Q., Dozier, J., Gillespie, T., Gu, Y., Kang, S. C., Piao, S. L., Sugimoto, S., Ueno, K., Wang, L., Wang, W. C., Zhang, F., Sheng, Y. W., Guo, W. D., Ailikun, Yang, X. X., Ma, Y. M., Shen, S. S. P., Su, Z. B., Chen, F., Liang, S. L., Liu, Y. M., Singh, V. P., Yang, K., Yang, D. Q., Zhao, X. Q., Qian, Y., Zhang, Y., and Li, Q.: Recent third pole's rapid warming accompanies cryospheric melt and water cycle intensification and interactions between monsoon and environment: Multidisciplinary approach with observations, modeling, and analysis, B. Am. Meteorol. Soc., 100, 423–444, https://doi.org/10.1175/BAMS-D-17-0057.1, 2019.

Yao, X. J., Liu, S. Y., Sun, M. P., Wei, J. F., and Guo, W. Q.: Volume calculation and analysis of the changes in moraine-dammed lakes in the north Himalaya: a case study of Longbasaba lake, J. Glaciol., 58, 753–760, http://dx.doi.org/10.3189/2012JoG11J048, 2012.

Yao, X. J., Liu, S. Y., Han, L., Sun, M. P., and Zhao, L. L.: Definition and classification system of glacial lake for inventory and hazards study, J. Geogr. Sci., 28, 193–205, https://doi.org/10.1007/s11442-018-1467-z, 2018.

Zemp, M., Huss, M., Thibert, E., McNabb, R., Huber, J., Barandun, M., Machguth, H., Nussbaumer, S. U., Gärtner-roer, I., Thomson, L., Paul, F., Maussion, F., Kutuzov, S., and Cogley, J. G.: Global glacier mass changes and their contributions to sea-level rise from 1961 to 2016, Nature, 568, 382–386, https://doi.org/10.1038/s41586-019-1071-0, 2019.

Zhang, G. Q., Yao, T. D., Xie, H. J., Wang, W. C., and Yang, Wei.: An inventory of glacial lakes in the Third Pole region and their changes in response to global warming, Glob. Planet. Change, 131, 148–157, http://dx.doi.org/10.1016/j.gloplacha.2015.05.013, 2015.

Zhang, G. Q., Bolch, T., Yao, T. D., Rounce, D.R., Chen, W. F., Veh, G., King, O., Allen, S.K., Wang, M. and Wang, W. C. Underestimated mass loss from lake-terminating glaciers in the greater Himalaya, Nat. Geosci., 16, 1–6. https://doi.org/10.1038/s41561-023-01150-1, 2023.

Zhang, T. G., Wang, W. C., Gao, T. G., and An, B. S.: Simulation and Assessment of Future Glacial Lake Outburst Floods in the Poiqu River Basin, Central Himalayas, Water, 13, https://doi.org/10.3390/w13101376, 2021.

Zhang, T. G., Wang, W. C., An, B. S., Gao, T. G., and Yao, T. D.: Ice thickness and morphological analysis reveal the future glacial lake distribution and formation probability in the Tibetan Plateau and its surroundings, Glob. Planet. Change, 216, 103923, https://doi.org/10.1016/j.gloplacha.2022.103923, 2022.

Zheng, G. X., Mergili, M., Emmer, A., Allen, S., Bao, A. M., Guo, H., and Stoffel, M.: The 2020 glacial lake outburst flood at Jinwuco, Tibet: causes, impacts, and implications for hazard and risk assessment, The Cryosphere, 15, 3159–3180, https://doi.org/10.5194/tc-15-3159-2021, 2021.